Extra- and intracellular ice formation in mouse oocytes, Cryobiology 51 (2005) 29–53]. Perhaps that is a reflection of their much larger size.

Keywords: Oocytes; *Xenopus laevis*; Freezing; Intracellular and extracellular; Plasma membrane

The most important single factor determining the success of cryopreservation is whether or not a cell undergoes intracellular ice formation (IIF) during freezing. In "classical" freezing, IIF is avoided by cooling cells sufficiently slowly so that osmotic dehydration results in their water remaining in near chemical potential equilibrium with the outside solution and ice. The faster the cooling, the more the cell water volume departs from equilibrium, and the more it departs from equilibrium, the more it is supercooled.

A supercooled cell will eventually freeze intracellularly at some sub-zero ice nucleation temperature or zone. Consequently, whether or not a cell freezes internally depends not only on the cooling rate, but also on the boundary temperature of the nucleation zone. The two factors interact. The higher the nucleation temperature, the lower the cooling rate has to be to ensure that the cell is sufficiently dehydrated by the time it reaches that temperature. If the nucleation temperature is too high, it would become impossible to achieve sufficient cell dehydration to avoid IIF no matter how low the cooling rate. In other words, it would become impossible to cryopreserve by classical slow freezing. Such appears to be the case in starfish oocytes [8] and zebrafish embryos [3].

Because of its central importance to cryobiology, we have initiated an in-depth study of factors that influence the temperature at which IIF occurs. The model cells chosen for study are mouse oocytes and oocytes of the frog *Xenopus laevis*. Information on the former was published recently [12,14]. The present report describes cryomicroscope studies on Stage I and II *Xenopus* oocytes. It complements another recent paper by Kleinhans et al. [7] reporting the results of intracellular freezing in Stage I to VI *Xenopus* oocytes by differential scanning calorimetry (DSC). An important mechanistic reason for selecting the oocytes of these two species is that while their plasma membranes do not normally possess aquaporin channels, it is possible to express aquaporin water channels in both. This allows a test of the hypothesis that one route of IIF may be the growth of external ice crystals through existing pores in the plasma membrane [10]. Before pursuing *Xenopus* as a model for aquaporin effects on IIF, the properties of wild type, non-expressing oocytes needs to be established. The current paper reports our cryomicroscope findings on these non-expressing oocytes.

Xenopus oocyte development is divided into six stages (I–VI). The maturation is accompanied by a six-fold increase in diameter from ~200 to 1200 μm and a conversion from transparency to opacity. For reasons of size and opacity, only Stage I and II (~300 μm) oocytes are amenable to cryomicroscopic observations. That limitation does not apply to DSC studies.

Methods

As just mentioned, a central aim of our research is to compare the ice nucleation behavior of control oocytes, which lack aquaporin channels, with that of oocytes in which these channels have been expressed.

Obtaining Xenopus Stage I and II oocytes

Mature female oocyte positive *X. laevis* frogs were obtained from *Xenopus* Express (Plant city, FL) and housed in tanks in The University of Tennessee, Knoxville animal facility. Oocytes were harvested as previously described [2] by surgical removal of oocyte sacks. Oocyte sacks were then defolliculated by treatment with 2 mg/ml collagenase type IA (Sigma No. C-9891) in filtered Ringers solution without calcium (96 mM NaCl, 2 mM KCl, 5 mM $MgCl_2$, and 5 mM Hepes–NaOH, pH 7.6) for 2–3 h at room temperature. Oocytes were periodically visually inspected during collagenase treatment to monitor follicular cell removal and to prevent over digestion [19]. Collagenase treatment was stopped by removal of collagenase by washing oocytes in filtered Ringers solution (96 mM NaCl, 2 mM KCl, 5 mM $MgCl_2$, 0.6 mM $CaCl_2$, 5 mM Hepes–NaOH, pH 7.6, 100 μg/ml pennicillin–streptomycin, and 5% [v/v] horse sera) until the solution turned clear (usually 4–5 washes, 40 ml each). Oocyte stages were determined by size and appearance according to Hausen and Riebsell [4] and separated into sterile 96-well microtiter plates (Falcon

No. 351177). Oocytes were cultured in filtered Ringers solution between 1 and 2 days at 16 °C before the experimental treatment.

Experimental media

Prior to freezing, the majority of oocytes were exposed at room temperature for 15–35 min in approximately 10 ml of Ringers solution supplemented with various concentrations of either ethylene glycol or glycerol (0, 0.5, 1.0 or 1.5 M). A sizeable number were exposed for shorter times (1–10 min), and a few for longer times (60 min). The composition of experimental media solutions is given in Table 1. In addition, the media used for freezing experiments also contained 10 mg/L of a commercial freeze-dried preparation of *Pseudomonas syringyii* (Snowmax) to induce the formation of extra-cellular ice (EI) at higher temperatures than would otherwise be the case.

Preparing the Linkam sample

The sample container for the Linkam cryostage used in our experiments (next section) consists of a shallow quartz dish 14 mm inner diameter and 2.56 mm deep. The bottom is 40 μm thick. A 250 μm thick washer measuring 12.7 mm OD and 7.9 mm ID was punched from plastic shim stock with Ted Pella disc punches #54743 and 54740, and placed in the quartz dish. Then, (1) A 4 μl drop of the test medium containing one to nine oocytes was pipetted into the center of the washer, and a 12 mm round glass cover slip (Ted Pella No. 26023) was applied with vacuum tweezers. (The purpose of the washer was to prevent distortion of the oocyte by the cover glass.) (2) The quartz dish was then quickly placed in the Linkam sample holder, which was then inserted into the Linkam stage and a freezing run immediately initiated. Approximately 1–2 min elapsed between initiating step (1) and completing step (2).

The Linkam cryostage

A BCS 196 cryostage (Linkam Scientific Instruments, Waterfield, UK) along with a Paxcam digital CCD camera (800 × 600 resolution) and Pax-it control and capture software (v. 6.1) developed by Midwest Information Services (Franklin Park, IL) for the Linkam, and integrated by McCrone Microscopes and Accessories (Westmont, IL) were used for these experiments. The cryostage was attached to a Zeiss bright-field microscope and the oocytes observed with an Olympus 6.3× (for Stage II oocytes) or 10× (for Stage I oocytes) long working distance microscope objective. The Pax-it software permits the setting of multiple ramps in which the variables are cooling rate (up to 50 °C/min), temperature limit, holding time at desired temperatures, and warming rate. Warming and cooling are effected, respectively, by electric heating and nitrogen vapor cooling of a silver control block. The maximum capture rate of 1 image/10 s was used during critical phases of the experiment. Images, however, are observed continuously in real time at 40 frames/s on the monitor.

The quartz dish referred to above rests on the silver cooling block. (Quartz has about twice the thermal conductivity of flint glass.) During a run, the temperature output of a thermocouple imbedded near the top of the cooling block is displayed continuously to 0.1 °C. We have several internal measures indicating that the sample temperature is quite accurately reflected by the displayed temperature. The first and most precise is that 2.5 μl of water spread into a thin film between two

Table 1
Initial composition of solutions

Solution	Wt % salt	Wt % CPA	R	Wt% water	m salt	m CPA	R'	M CPA	MP (°C)
XR0-1X	0.6	0	0	99.4	0.104	0	0	0	−0.4
XR8-1X-G5	0.57	4.53	7.87	94.88	0.104	0.52	4.99	0.5	−1.35
XR15-1X-G8	0.55	8.1	14.59	91.34	0.104	0.96	9.25	0.9	−2.17
XR16-1X-G9	0.55	8.98	16.35	90.49	0.104	1.07	10.37	1	−2.39
XR25-1X-G13	0.52	13.34	25.48	86.28	0.104	1.68	16.17	1.5	−3.5
XR5-1X-EG3	0.58	3.07	5.25	96.34	0.104	0.515	4.95	0.5	−1.35
XR11-1X-EG6	0.56	6.13	10.81	93.3	0.104	1.059	10.18	1	−2.36
XR17-1X-EG9	0.54	9.16	16.7	90.28	0.104	1.636	15.73	1.5	−3.43

R is the wt% CPA/wt% salt. R' is the mole ratio CPA/salt. XR0-1X is frog Ringers solution (as described under Methods) with the concentrations expressed as NaCl equivalents. In column 1, EG, ethylene glycol; G, glycerol; m, molal concentration; M, molar concentration; MP, melting point; all solutions also contained 10 mg/L Snowmax.

12 mm cover slips is observed to melt during warming at 10 °C/min at a displayed temperature of −0.2 to 0 °C. Second, all the experiments involved an initial warming ramp of a seeded sample to a displayed ~1 °C below the melting point of the test solution. As expected, most, but not all of the ice, is observed to have melted at the upper limit. Third, since Ringers is primarily NaCl (96 mM), melting during warming is expected to begin slightly below the eutectic point of pure NaCl, which is −21.1 °C. That in fact was observed. Fourth, when 4 μl droplets of oocytes in CPA/Ringers undergo their final warming and thawing at 10 °C/min, the last traces of ice vanish at an indicated 3–3.5 °C above the computed melting point. That is in accord with our experience with calibrated thermocouples imbedded in small volumes of solution warmed at comparable rates.

Video taping

In a number of experiments, the Pax-it acquired images were supplemented with digital video recordings. These DVs permitted the acquisition of images at 0.03 s resolution (the precise scan rate being 29.97 images/s). The images were obtained by photographing a supplementary LCD monitor screen with a Sony DCR-TRV 38 digital video camera recorder. Relevant portions of the resulting tape were captured on computer using U-Lead Video Studio 7 software (www.ulead.com).

Statistics

Plus/minus values in tables and figures are standard errors (standard deviations of the mean). Tests of statistical significance were carried out by a two-tailed Student's *t* test and two-way ANOVA using Graph Pad's (San Diego) Prism.

Results

Stage I and II oocytes were visually inspected for obvious signs of membrane damage under a dissecting scope before loading into the Linkam stage. After loading onto the Linkam stage, the oocytes were again visually examined to exclude those with clearly abnormal morphology or obvious signs of membrane damage such as "blebbing."

In experiments where EG or glycerol were used, the oocytes underwent a rapid decrease in volume manifested as a slightly crumpled appearance. This was a consequence of the osmotic withdrawal of intracellular water. This was followed by a more gradual re-expansion to an extent depending on the exposure time to CPA. We return to this point later in Results.

Ramps

The typical program for examining IIF for oocytes employed 6 thermal ramps as shown in Fig. 1 and Tables 2 and 3. The lower limit for Ramp 2 was set approximately 1 °C below that predicted for extracellular freezing (Table 3). The incorporation of a warming ramp (Ramp 3) just after extracellular freezing melted most of the external ice and served three purposes: (1) as an internal control of the accuracy of the thermocouple readings. (2) It allowed the oocytes to become clearly visible so that the morphological effects of the external ice formation could be assessed. (3) The melting of the majority of external ice during Ramp 3 served to equilibrate the chemical potentials of water inside

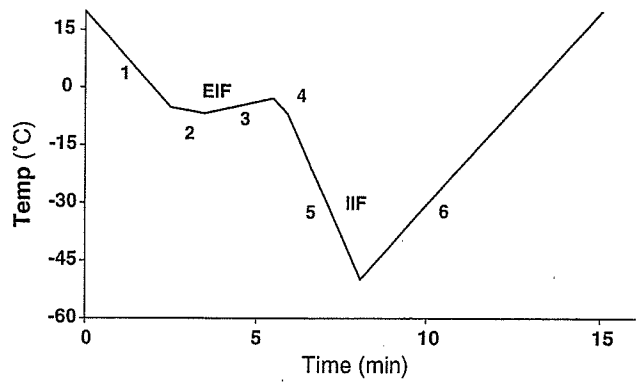

Fig. 1. Schematic of Linkam cryostage thermal ramp program for oocytes in 1 M EG/Ringers. Individual ramps corresponding to those in Table 2 are labelled sequentially. EIF occurs in Ramp 2 and IIF usually occurs in Ramp 5.

Table 2
Linkam cryostage cooling and warming ramps for *Xenopus* oocytes in 1 M CPA

Ramp No.	Rate (°C/min)	Limit (°C)	Capture interval (s)	Comments
1	10	−5.0	30	Cooling
2	2	−7.0	10	Cooling; EIF
3	2	−2.8	10	Warming; partial thawing
4	10	−7.0	10	Cooling
5	10	−50.0	10	Cooling; IIF
6	10	+20.0	30	Warming and thawing

With the exception of the limit temperatures in Ramps 2–3 (see Table 3), most of the other entries were the same or similar in other concentrations of CPA.

Table 3
Limits for initial cooling in Linkam cryostage Ramp 2 and warming in Ramp 3, and observed EIF and supercooling in the various concentrations of freezing solutions

Solution	M CPA	Ramp 2 limit (°C)	Observed EIF (°C)	Calc. MP (°C)	Supercooling at EIF (°C)	Ramp 3 limit (°C)
XR0-1X	0	−5.2	−3.87 ± 0.03	−0.4	−3.47	−0.2
XR8-1X-G5	0.5	−6.0	−5.17 ± 0.02	−1.35	−3.82	−2.8
XR16-1X-G9	1	−7.0	−6.50 ± 0.00	−2.39	−4.11	−2.8
XR25-1X-G13	1.5	−9.0	−7.99 ± 0.06	−3.5	−4.49	−4.5
XR5-1X-EG3	0.5	−6.0	−5.10 ± 0.03	−1.35	−3.75	−1.7
XR11-1X-EG6	1	−7.0	−6.33 ± 0.09	−2.36	−3.97	−2.8
XR17-1X-EG9	1.5	−9.0	−7.67 ± 0.07	−3.43	−4.24	−3.8

and outside the oocyte before cooling Ramps 4 and 5. In other words, the oocytes were minimally supercooled at this stage.

Ramps 1, 4–6 remained essentially the same for all the concentrations of glycerol and EG studied, but the limits for Ramps 2 and 3 depended on the solution as summarized in Table 3. Table 3 also depicts the mean observed temperatures of EIF, and the calculated thermodynamic melting points of the solutions. The latter were calculated as −1.855× the molality of the CPA minus the 0.4 °C melting point depression of isotonic Ringers. (1.855 is the so-called molal freezing point constant). The molalities of CPA are given in Table 1.

Most of the experiments used a cooling rate of 10 °C/min in Ramp 5.

Extracellular freezing

EIF occurred when the solutions were supercooled an average of 3.5 °C (Ringers), 3.8–4.5 °C (glycerol), and 3.8–4.2 °C (EG) below the thermodynamic freezing (melting) points (Table 3). The relatively small amount of supercooling was a consequence of the presence of catalytic quantities of freeze-dried ice-nucleating bacteria (Snomax).

EIF was manifested by dendritic spears of ice apparently being projected at high rate (~800 μm/s) across the field of view (Fig. 2B). Projected spears are of course illusory; rather, they are akin to the propagation of a crack in window glass. The initial spears exert no evident force on the oocytes other than a small shift or rotation of the eggs as they are displaced slightly by the developing ice phase.

Immediately thereafter, the thickening extracellular ice in Ramp 2 mostly or totally obscures the fine details of the oocytes. The obscuration was greater with increasing concentrations of CPA.

Oocyte distortion from EIF

The oocytes become visible again at the end of the transient warming in Ramp 3 when most of the external ice has melted. Examination of the *Xenopus* oocytes during this stage showed no apparent distortion in marked contrast to that observed for mouse oocytes [14]. Examples are shown in Fig. 2D for *Xenopus* oocytes.

Plasma membrane integrity was manifested by the fact that intracellular ice formation (IIF) as evidenced by "flashing" did not occur in the majority of oocytes (see next section) until well into Ramp 5 at temperatures often far below EIF. In the region between EIF and IIF, the water in the oocytes had to be supercooled and the only way for supercooled water to co-exist with surrounding ice is to be separated from that ice by an intact plasma membrane.

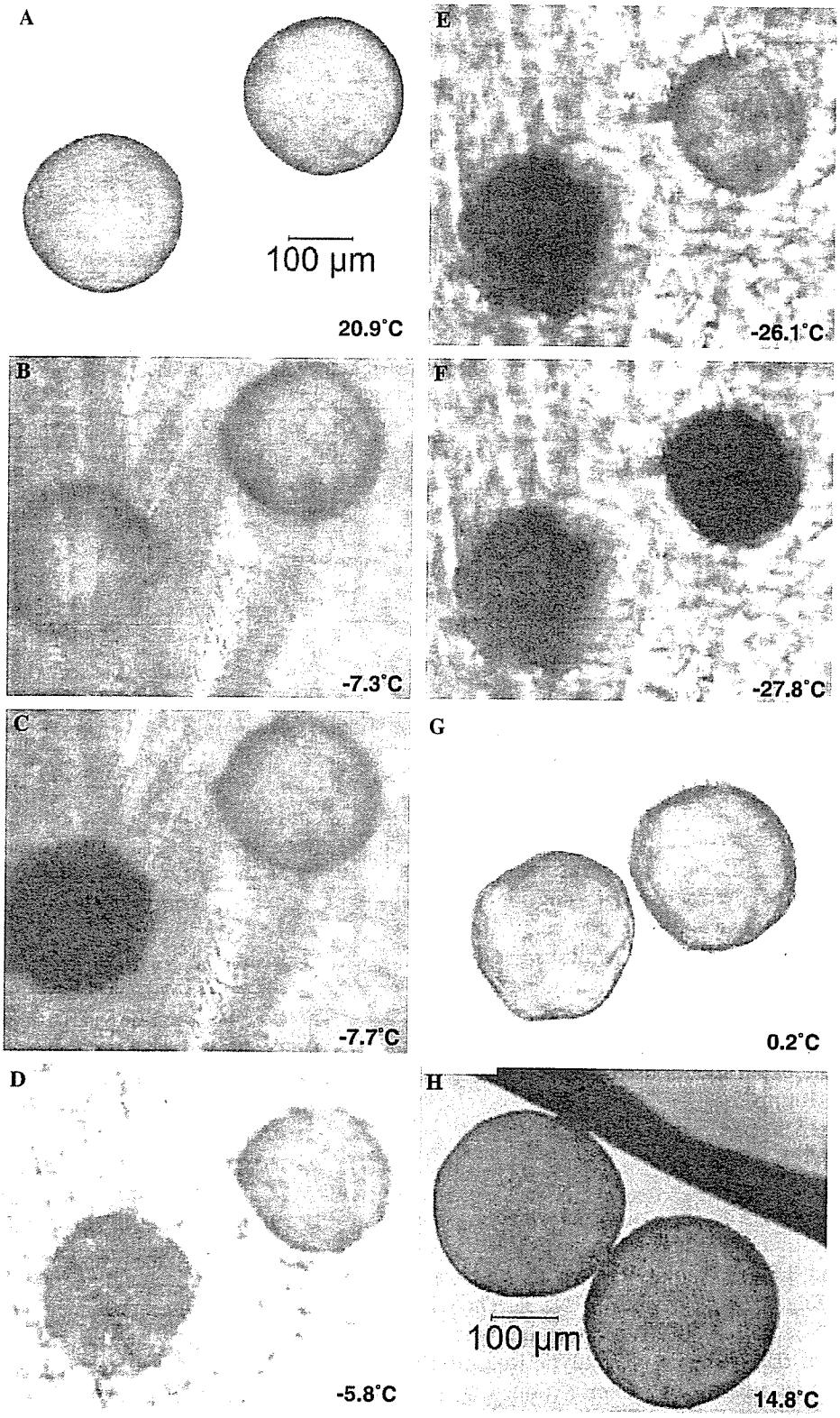

Fig. 2. Photomicrographs of a representative Linkam freezing experiment of two Stage I oocytes. Oocytes suspended in 4 µl of 1.5 M EG/ringers were subjected to a Linkam thermal program similar to that depicted in Fig. 1 (see Tables 2 and 3). (A) Initial oocyte observation (Ramp 1), (B) EIF (Ramp 2), (C) the high-temperature flashing of one oocyte (Ramp 2), (D) partial melting of extracellular ice (Ramp 3), (E) rapid cooling (Ramp 5), (F) low-temperature flashing of the second oocyte (Ramp 5), (G) oocytes after melting of external ice (Ramp 6), (H) oocytes at the end of Ramp 6. Temperatures are displayed in the lower right-hand corner of each individual panel.

In the case of about half the oocytes, the EIF and/or the consequent distortion did disrupt or damage the plasma membrane as evidenced by either the total lack of flashing (which we interpret as an inability to supercool) or by flashing at temperatures very close to the EIF temperature. We elaborate on these points in the next section.

High and low temperature flashing

As mentioned above, a significant number of the *Xenopus* oocytes assayed flashed close to the temperature at which EIF occurred. Fig. 2 shows two representative oocytes from a single freezing run in the Linkam cryostage with 1.5 M EG cryoprotectant. The oocyte on the left flashed at −7.7 °C, close to the EIF temperature of −7.3 °C. (Figs. 2C and B). We refer to these as "high temperature flashers." In contrast, the oocyte in the upper right hand corner flashed at −27.8 °C (Fig. 2F) and is placed in the "low temperature flashers" category. The distribution of oocytes into these two categories becomes apparent when graphing the number of oocytes which flashed at a given temperature vs. temperature (Fig. 3). In the case of freezing runs conducted in the presence of 1.5 M EG, the biphasic distribution of oocyte flashing is clear.

The frequency distributions for the IIF of oocytes in Frog Ringers alone and in the other concentrations of CPA used is summarized in Fig. 4. An arrow shows the mean EIF for that solution.

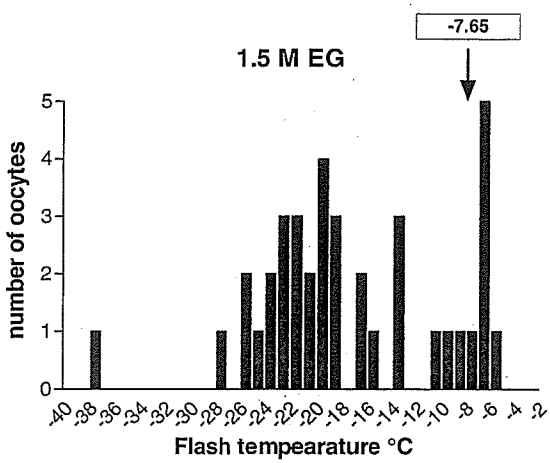

Fig. 3. Biphasic distribution of flash temperatures of oocytes suspended in 1.5 M EG. Vertical bars represent the number of oocytes displaying flashing at a given temperature in 2 °C increments. The mean EIF temperature (°C) for 1.5 M EG/Ringers is shown by the upper right-hand value and arrow.

As can be seen, the distribution tends strongly to be bimodal. In each case, one group of oocytes flashed at temperatures near the mean EIF; the other group flashed at temperatures well below EIF. Table 4 gives the fraction that fell into each category for the different solutions. For purposes of this table, we include in the high-temperature category, those that flashed less than 1.5 °C below EIF and the few that flashed above the EIF temperature during the warming phase of Ramp 3.

Note that in Figs. 3 and 4 that there are five oocytes out of the total of 114 that flashed at −38 °C or −40 °C. This is at or close to the homogeneous ice nucleation temperature for objects the size of these eggs (see Discussion).

For all subsequent data analysis, the high temperature flashing oocytes were excluded since this behavior would seem to indicate plasma membrane damage either associated with the earlier EIF ramps or with the collection and pre-freezing manipulations.

Intracellular ice formation in the low-temperature flashers

The fourth column of Table 5 summarizes the temperatures at which Stage I and II oocytes underwent IIF (flashing) as a function of the CPA present [none (i.e., Ringers only), glycerol, and EG] and its concentration (0.5–1.5 M). There is a marked decrease in the mean flashing temperature with increased CPA concentration; namely, from −11.4 °C in Ringers alone to −29.4 °C in 1.5 M glycerol/Ringers and −21.1 °C in 1.5 M EG/Ringers. Comparison of the effects of increasing concentrations of both glycerol and EG show that glycerol exerts little or no effect on depressing the flash temperature at concentrations between 0 and 1 M but a sizeable effect between 1 and 1.5 M, while EG shows an initial effect between 0 and 0.5 M concentrations and no effect between 0.5 and 1.5 M (Fig. 5). [The differences in flash temperatures between 0.5 M EG and 0.5 M glycerol and between 1.5 M EG and 1.5 M glycerol are significant ($p < 0.001$)].

IIF in Stage I vs. Stage II oocytes

Fig. 6 compares the mean flash temperatures of Stage I and II oocytes in the various media. There is no statistically significant effect of stage ($p = 0.9$). Hence, the data for both stages presented in Table 5 and later have been pooled.

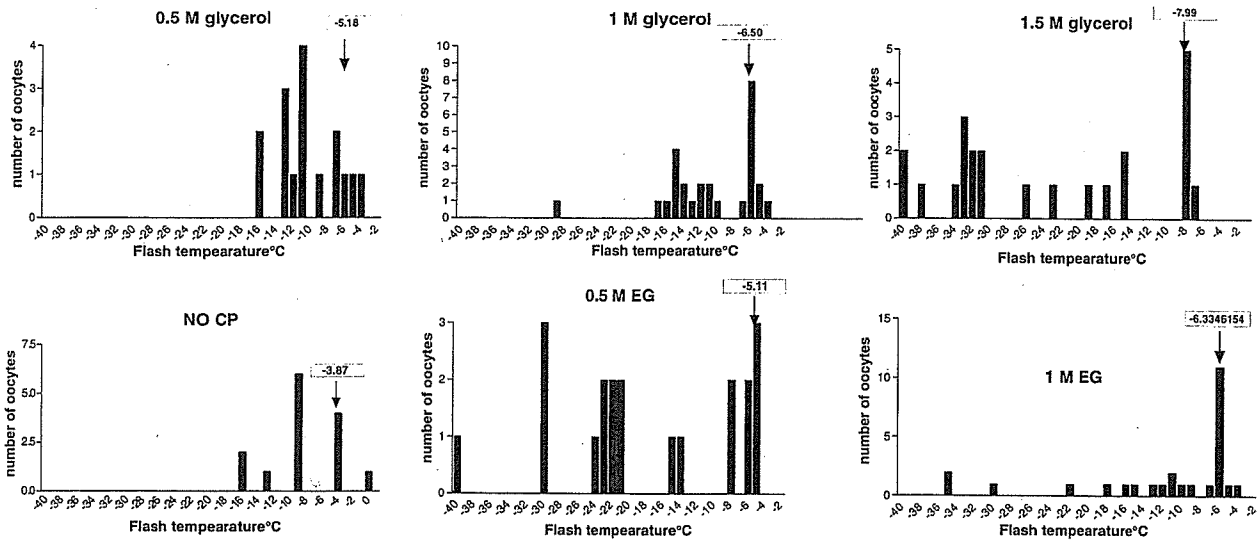

Fig. 4. Distribution of flash temperatures of oocytes suspended in 0.5 or 1.0 M EG, 0.5, 1.0 or 1.5 M glycerol, and Frog Ringers lacking CPA. The arrows depict the mean EIF temperatures.

Table 4
High temperature flashers vs. low temperature flashers

CPA	M CPA	n	% High flashers	% Low flashers
—	0	14	36	64
Glycerol	0.5	16	19	81
Glycerol	1	27	41	59
Glycerol	1.5	23	26	74
EG	0.5	19	16	84
EG	1	27	52	48
EG	1.5	38	21	79

IIF vs. CPA permeation

The movement of a permeating solute like EG or glycerol into a cell is manifested in two ways. First, the volume of the cell decreases rapidly as intracellular water is rapidly removed and then returns towards normal as the solute permeates. The second manifestation of permeation is that the concentration of CPA rises very rapidly to near the equilibrium concentration and then asymptotes slowly to the equilibrium concentration. The

Table 5
Effect of CPA type and concentration on the flash temperature of *Xenopus* oocytes and the characteristics of the unfrozen channels at the flash temperature

Solution	CPA	Molarity	Flash temperature (°C)	n	L at flash	U at flash	R	R'	m_s at flash	m_{CPA} at flash
XR0-1X	None	0	-11.4 ± 1.0	9	0.043 ± 0.003	0.037 ± 0.003	0	0	2.96	0
XR8-1X-G5	Glycerol	0.5	-12.2 ± 0.8	13	0.158 ± 0.006	0.113 ± 0.006	7.87	4.99	0.95	4.65
XR16-1X-G9	Glycerol	1	-15.2 ± 1.1	16[a]	0.254 ± 0.010	0.177 ± 0.011	16.35	10.37	0.62	6.43
XR25-1X-G13	Glycerol	1.5	-29.4 ± 2.0	17	0.251 ± 0.011	0.140 ± 0.013	25.48	16.17	0.76	12.28
XR5-1X-EG3	EG	0.5	-21.0 ± 2.3	16	0.101 ± 0.002	0.067 ± 0.002	5.25	4.95	1.66	8.22
XR11-1X-EG6	EG	1	-18.7 ± 2.6	13	0.198 ± 0.003	0.141 ± 0.003	10.81	10.18	0.79	8.04
XR17-1X-EG9	EG	1.5	-21.1 ± 0.1	30	0.307 ± 0.002	0.233 ± 0.002	16.7	15.73	0.45	7.08

L is the fractional mass of the solutions that remain unfrozen; U is the fractional mass of unfrozen water. L, U, and m_s values were calculated for each flash temperature, averaged, and the standard deviations of the mean calculated. R is wt % CPA/wt % salts. R' is moles CPA/moles salts.

[a] The results of these 15 oocytes include, six that were analyzed using 0.9 M glycerol/Ringers instead of 1.0 M.

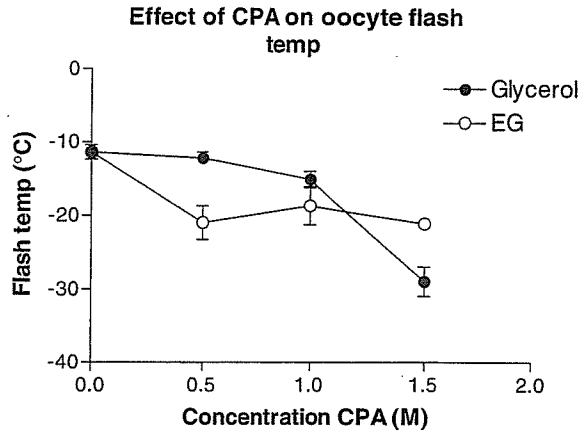

Fig. 5. Effect of CPA on oocyte flash temperature. Oocyte flash temperatures vs. concentrations of glycerol (closed circles) and EG (open circles).

"shrink-swell" behavior is illustrated for *Xenopus* Stage II oocytes in 1.5 M EG (Fig. 7A) and 1.5 M glycerol (Fig. 7C). The second manifestation, the rapid rise in intracellular concentration, is illustrated in Figs. 7B and D. The values used to make these computations were $V_b = 0.15$; $L_p = 0.73$ μm/min/atm; $P_{EG} = 0.0012$ cm/min; $P_{gly} = 0.0003$ cm/min. To elaborate, Kleinhans et al. [6] have measured the swelling rate of Stage I and II oocytes in hypoosmotic frog Ringers, and using standard water permeability equations, they determined which calculated swelling curves provided the closest match to the experimental curves using L_p (hydraulic conductivity) and V_b (non-osmotic volume of the cell) as adjustable parameters in the calculations. The best fits were obtained with $V_b = 0.15$ and $L_p = 0.73$. Edashige et al. (unpublished) have made analagous measurements on Stage V oocytes, except they obtained the value of V_b directly by extrapolating a Boyle–van't Hoff curve to infinite solute concentration. The value they obtained, $V_b = 0.69$ is nearly 5-fold higher than Kleinhans et al.'s and that is consistent with the much higher yolk content of the Stage V egg vs. the Stage I or II. Their value of L_p was similar to that of Kleinhans et al. [6]. There are no measurements in the literature for the permeability of Stage I and II oocytes to EG and glycerol; consequently, we used the values reported by Edashige for Stage V; namely $P_{EG} = 0.0012$ cm/min and $P_{gly} = 0.0003$. Our rationale was that if the L_p's are the same in early and late stages, the membrane properties to EG and glycerol are probably similar.

The majority of the oocytes here were exposed to CPA for 15–60 min. Figs. 7A and B indicate that in 1.5 M EG for that time interval their volumes would have increased to 72–96% of normal and the internal EG concentration would have equilibrated. Some were exposed for times as short as 2 or 5 min. The same figures illustrate that their volumes would have been near minimum, but the internal EG concentration would be 75–97% of equilibrium. In 1.5 M glycerol (Figs. 7C and D), both the oocyte volumes and the internal concentration of glycerol would have been much lower than in EG for given exposure times because of the 4-fold lower permeability coefficient.

Experimentally, however, we see no significant difference in mean flash temperature regardless of

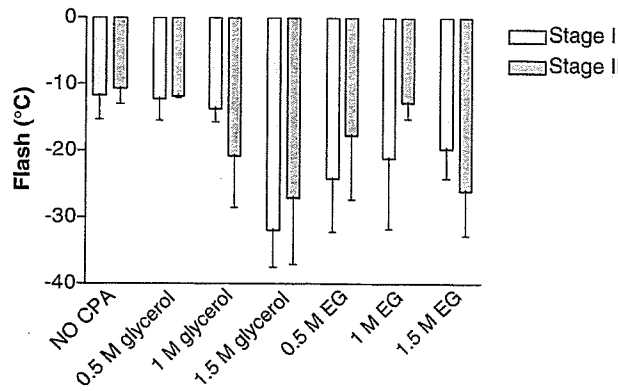

Fig. 6. Flash temperatures of Stage I vs. Stage II oocytes. Oocyte flash temperatures of the low flasher oocytes as measured in Ringers alone or in Ringers supplemented with CPA.

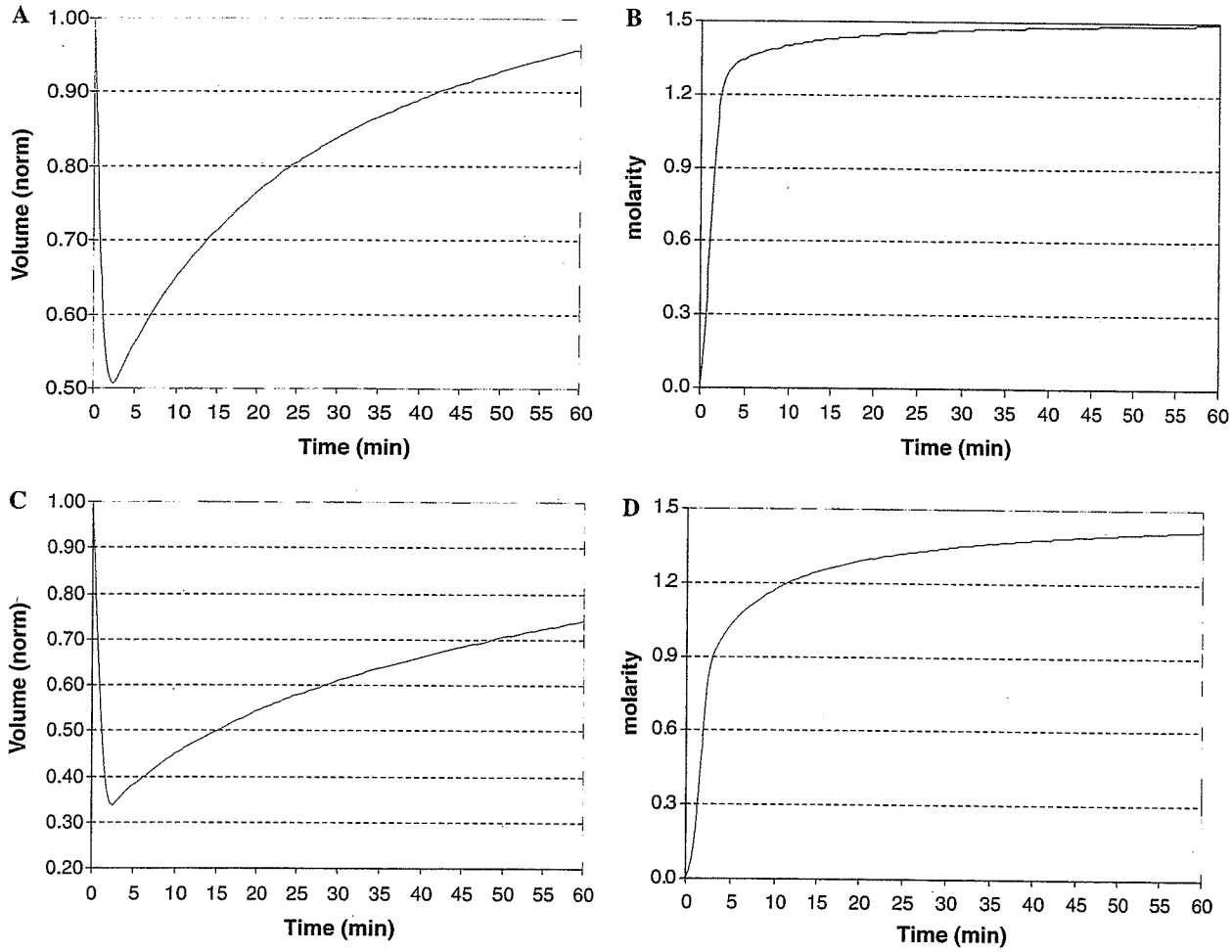

Fig. 7. Calculated equilibration rates for Stage II oocytes. (A) Computed relative volumes of Stage II oocytes as a function of time in 1.5 M EG. (B) Computed intracellular concentration of EG as a function of time in 1.5 M EG. (C) Computed relative volumes of Stage II oocytes as a function of time in 1.5 M glycerol. (D) Computed intracellular concentration of glycerol as a function of time in 1.5 M glycerol (see text for the values used in the computations).

exposure time to CPA or regardless of whether the CPA was EG or glycerol.

Oocyte re-freezing

To further examine the properties of the *Xenopus* oocyte plasma membrane after IIF, we subjected four oocytes to a second set of thermal ramps identical to the first. Interestingly, it was noted that oocyte "flashing" during these repeat runs coincided with the initial EIF of Ramp 2. This is a strong indication that the IIF that occurred during the first freezing run caused some type of defect or damage in the plasma membrane which negates its normal ability to prevent IIF upon initial contact with extracellular ice.

Composition and physical characteristics of the unfrozen medium at the instant of flashing

As extracellular ice develops during cooling, water is progressively removed from the solution and transformed into ice. Cells are located in the unfrozen channels between the growing ice crystals. With lowered temperature, these channels diminish in size, and the concentration of solutes in them increases. Both the fractions that remain unfrozen at the flash temperature and the concentration of salts and CPA in those channels can be calculated from phase diagrams. Columns 6–11 of Table 5 summarize these quantities. The data for glycerol/NaCl/water and EG/NaCl/water are calculated from ternary phase relations published by Pegg

[17] and Woods et al. [26], respectively. Pozner et al. [18] have shown that the phase relations of glycerol/physiological saline/water are essentially indistinguishable from those of glycerol/NaCl/water.

The procedure is as follows: the phase diagrams depict the freezing or melting points as a function of the total weight percent (W_T) of CPA + salt. The position of the curves (or isopleths) depends on R, the weight ratio of CPA/salt. Equations published by the two groups permit one to calculate W_T for a specified R and subzero temperature. For glycerol/NaCl/water solutions, Pegg's equation is

$$W_T = a + (a^2 - 0.04T_{fl})^{1/2}/0.02,$$

where $1/a = -1/.6 - 1.27R - 0.25R^2$ and T_{fl} is the flash temperature.

For EG, rearrangement of Woods et al.'s equation 3 yields

$$W_T = (-b - (b^2 - 4ac)^{1/2})/2a,$$

where:

$$b = -0.676 + (4.77E - 03)R,$$

$$a = (-7.64E - 03) + (-2.75E - 05)R,$$

$$c = -T_{fl}.$$

From knowledge of R, W_T, and W_T^0, the total weight percent of CPA and salt in the solution prior to freezing (see Table 1), one can compute the values shown in Table 5. L is the weight fraction of the original solution that remains unfrozen at the specified flash temperature. It is calculated as W_T^0/W_T. U is the weight fraction of the water in the unfrozen solution that remains unfrozen at a specified temperature. It is calculated from Eq. (7) of Rall et al. [20]; namely

$$U = (100 - W_T)L/(100 - W_T^0).$$

We see from Table 5 that the unfrozen fraction of solution (L) exceed those of the unfrozen fraction of water (U) at a given flash temperature, because the former includes the mass or volume occupied by the CPA and salt molecules. Consequently, the differences between the two measures increase as the concentration of CPA increases Figs. 8A and B plot the values of L and U, respectively,

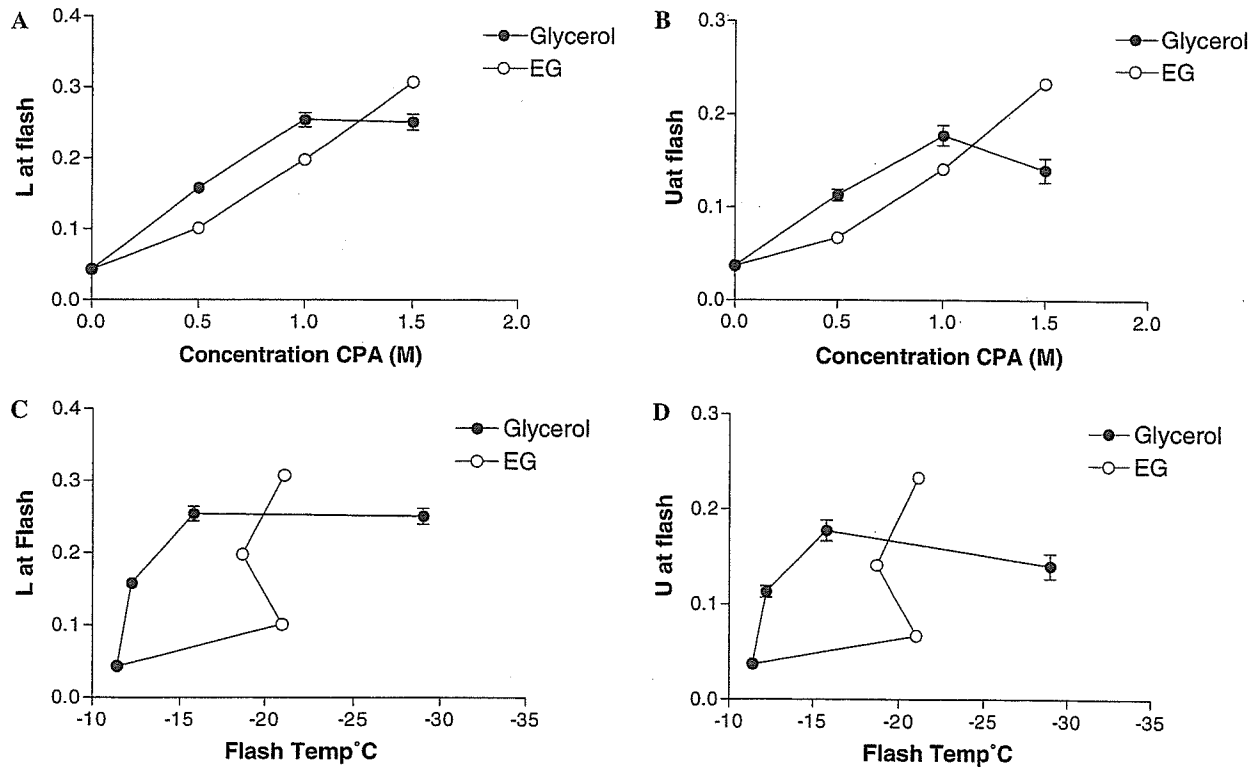

Fig. 8. Characteristics of the solution upon oocyte flashing. (A) fractional mass of unfrozen solution (L) at the moment of oocyte flashing as a function of the CPA concentration. (B) Fractional mass of the unfrozen water (U) at the moment of flashing as a function of CPA concentration. (C) L at the flash temperature as a function of the flash temperature. (D) U at flash temperature as a function of the flash temperature.

at the flash temperature as a function of the CPA concentration, and Figs. 8C and D the values of L and U at the flash temperature as a function of the flash temperature. If a critical value for the unfrozen fraction were the major determinant of the flash temperature, one would expect that the values of L and U at the flash temperature would be similar irrespective of the CPA concentrations and irrespective of the flash temperatures; i.e., the plots would approximate horizontal lines. Clearly that is not the case.

The quantities m_s and m_{CPA} in Table 5 are the molalities of salt and CPA in the unfrozen solution at the flash temperature. The former is calculated from Rall et al.'s [20, Eq. (7)]; namely

$$m_s = 1000W_s/[58.44(100 - W_T],$$

where W_s is the weight of salts in solution at the flash temperature, equals $W_T/(1 + R)$.

The m_{CPA} is $R' \times m_s$, where R' is the mole ratio of CPA/salt. That mole ratio is assumed to remain unchanged as freezing progresses. The salts and CPA concentrate simultaneously because pure water is being pulled out of the solution and converted to ice. The molality of salts at the flash temperature varies nearly 6-fold from 0.5–3 molal. The molality of CPA at the flash temperature varies 2.6-fold from 4.6–12 molal. If m_s or m_{CPA} were the critical determinant of the flash temperature, one would expect flashing to occur at a given molality of salt or CPA. That also is not the case.

All the flash temperatures occur well above the eutectic points for the ternary system glycerol/NaCl/water. From Eqs. (5) and (6) of Pegg [17], the eutectic temperatures are −62.0 and −67.3 °C for 0.5 M glycerol and 1.0 M glycerol in isotonic saline. Theoretically, there is no liquid present below those temperatures. The eutectic point of EG/water is −51 °C [15]. We know of no data for EG/NaCl/water.

These findings and conclusions with respect to unfrozen fractions relate to the overall fraction of liquid in the sample as derived from the phase diagrams. We have no information on the microstructural distribution of that unfrozen fraction, and in particular what microstructural environment of ice and unfrozen medium a given oocyte "sees" at the instant of its flashing. On the other hand, the micro environment that a given oocyte sees with respect to the concentrations of CPA and salt should be close to the global values derived from the phase diagrams.

Point origin of flash

Videotapes were made of 13 runs. In 11 of those runs, flashing occurred in a directional manner from a single point of origin near the surface. An example of this is shown in Fig. 9. It took 10 ms from the

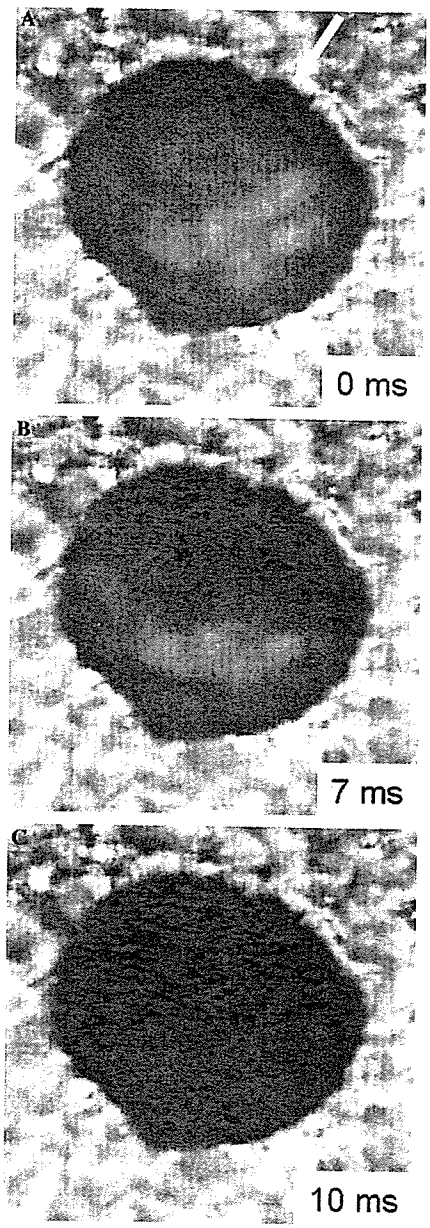

Fig. 9. Oocyte directional flashing. Video images of a Stage I$^+$ oocyte in 1.5 M EG/Ringers displaying directional flashing were captured as described under Methods. The first frame where the onset of flashing becomes apparent is depicted as 0 ms, and the starting point and direction of the flashing event is indicated by an arrow. The onset of flashing occurred at −28.2 °C.

start of blackening to its completion, a propagation rate of ~20,000 μm/s.

Manifestations of injury after thaw

Xenopus oocytes that had undergone flashing did not display gross distortion of their internal structure or their plasma membranes immediately after thawing in Ramp 6, other than some minor blebbing in some cases. However, they did manifest signs of injury in the form of an abrupt increase in volume by as much as 50% over normal by the time they had warmed to 15 or 20 °C. (Compare Figs. 2A and H). Swelling after IIF also occurs in mouse embryos [5] and oocytes (Mazur et al., unpublished).

Discussion

Lack of visible distortion at end of the warming in Ramp 3

Recall that after EIF occurs in Ramp 2, the oocytes are warmed to just below the thermodymamic melting point of the solution in Ramp 3. This melts most of the external ice and allows the oocytes to be seen clearly. In mouse, the oocytes are usually considerably distorted at this point, presumably as a consequence of being forced between the growing external ice crystals [14]. But that is not so for Stage I and II *Xenopus* oocytes in spite of their having about 3× and 5× the diameter and 27× and 125× the volume of the mouse egg. We do not know the explanation of the difference. Perhaps it is related to the fact that *Xenopus* oocytes possess a complex cortical array of microfilaments, microtubules, and intermediate filaments that confer high structural stability to the eggs [24].

High and low temperature freezers

In the Linkam observations, flashing falls into two groups, In one group, which we refer to as high-temperature flashers, it occurs within 1.5 °C of EIF; in the other group it occurs at temperatures further below EIF, usually well below. These we refer to as low-temperature flashers. The percentages in each group in the various media were summarized in Table 4. Kleinhans et al. [7] have reported a similar division into the two groups based on DSC measurements of oocytes in 1, 1.5, and 2 M EG. Pooled data for Stages I and II underlying their Fig. 5 show that 56% of oocytes in 1 M EG were high temperature freezers based on exotherms vs. our value in Table 4 of 52% based on visual flashing, and 32% of oocytes in 1.5 M EG were high temperature freezers vs. our value of 21%. One difference between their data and ours is that they show a substantially lower percentage of high temperature freezers in Stage I oocytes than in Stage II. We did not observe this difference.

This is very different behavior from the mouse egg [14]. There, high-temperature flashing is a rare event for eggs in CPA (7% of eggs in 1 and 1.5 M EG or glycerol).

What is responsible for the much higher percentages of high-temperature freezers in *Xenopus* is unknown. One possibility is that individual eggs vary in the stability of their plasma membranes to the physical or chemical forces exerted during EIF. This could either be an inherent variation, or subtle defects, or damage induced by the collection procedures (e.g., collagenase treatment), or less likely, pre-freezing manipulations. An alternative possibility, is that physical interactions between an individual oocyte and the surrounding EI varies in individual cases, perhaps because their excluded volume is much larger than in the case of the mouse. One observation that favors the latter is that of Kleinhans et al. [7] that by the time the oocytes reach the much larger Stage V and VI (~1200 μm in diameter), over 90% fall in the high temperature group. (As we have indicated, oocytes beyond Stage II can not be visualized on the Linkam cryo stage.)

In a few cases, the high-temperature flashing occurred above the EIF temperature (See Fig. 4); i.e., during warming in Ramp 3. This we interpret as being a time effect rather than a temperature effect.

Flash temperature vs. permeation of CPA

We found no significant effect on the flash temperature of oocyte volume or intracellular CPA concentration prior to the initiation of freezing. These factors were influenced by the exposure time to CPA and by whether the CPA was EG or glycerol, the former having four times the permeability of the latter. This is similar to the findings for mouse oocytes [14].

IIF-Linkam vs. DSC

Table 6 compares the IIF temperatures observed here in terms of flashing using the Linkam with

Table 6
Flash temperatures: mouse vs. *Xenopus* oocytes

M CPA Ringers or PBS base	Flash temperature (°C) (observed)			T_h (°C) (calculated)	
	Mouse	*Xenopus* Linkam (I and II)[a]	*Xenopus* DSC (I and II)[a]	Mouse[c]	*Xenopus*[b]
0	−13.9[a]	−11.4	—	−37	−35
0.5 Gly	−30.8	−12.2	—	−39	−37
1 Gly	−41.3	−15.2	—	−41	−39
1.5 Gly	—	−29.4	—	−43	−41
0.5 EG	−24.8	−21.0	—	−39	−37
1 EG	−37.2	−18.6	−18.7	−41	−39
1.5 EG	−40.8	−21.0	−23.0	−43	−41

[a] Excludes cases where IIF was less than 1.5 °C lower than EIF.
[b] Homogeneous nucleation temperature, based on the data of Angell [1] for water vs. volume and including the suppression by CPA.
[c] Rall et al. [21].

those observed by Kleinhans et al. [7] in the same solutions in terms of exotherms in the DSC. The agreement between the two methods is excellent. The agreement provides strong evidence that intracellular flashing is indeed a manifestation of intracellular ice formation. The table also compares the Linkam data observed here in *Xenopus* oocytes with those observed in mouse oocytes by Mazur et al. [14], which we shall discuss shortly.

Flash temperatures in relation to homogeneous and heterogeneous nucleation

In the absence of foreign nucleating agents, water in bulk volume nucleates at −32 °C (1). This is the homogeneous nucleation temperature, T_h. T_h decreases with decreasing volume of the water sample and it decreases with a lowering of the thermodynamic melting/freezing point of the solution by the presence of solutes. The rule-of-thumb is that the nucleation temperature is decreased by ~2× the suppression of the melting point [22]. When nucleation occurs above the homogeneous temperature, it is believed to be induced by foreign nucleating agents and is referred to as heterogeneous nucleation.

We estimate the mean volume of water in Stage I and II *Xenopus* oocytes to be 7×10^6 and 2.3×10^7 μm^3. We have fitted Angell's data of T_h vs. water volume to be $T_h = -40.957 + 3.5743 \times X - 0.3286 \times X^2$, where X is the log of the diameter of the water drop. This equation yields a T_h of −34.3 and −34.0 °C for the volume of water in Stage I and II oocytes, or a mean T_h of −34.15 °C. If we apply Rasmussen and MacKenzie's conclusion that supercooling is suppressed twice the melting point suppression, the result is that T_h for that volume of Frog Ringers, 0.5, 1, and 1.5 M CPA-Ringers is −35.0, −37.0, −39.0, and −41.1 °C, respectively.

As mentioned in Results, five of the 114 low-temperature flashing oocytes flashed at −38 or −40 °C; that is, they underwent IIF at T_h, and therefore one can conclude they nucleated homogeneously, by which is meant they formed internal ice as a consequence of the spontaneous aggregation of sufficient water molecules to constitute a critically sized ice nucleus. The corollary is that these five oocytes contained no heterogeneous nucleators, by which is meant they contained no agents or particles capable of inducing ice nuleation. The detailed data underlying the report of Kleinhans et al. [7] show that almost exactly the same fraction of Stage I and II oocytes frozen in 1 or 1.5 M EG exhibited exotherms in the DSC at or below −38 °C (namely, 6/130 or 5%).

All the other 109 low temperature flashers (and the other 124 oocytes in the Kleinhans et al. [7] DSC study) underwent IIF well above T_h (Table 6), and one can conclude, therefore, that they nucleated heterogeneously. It seems to us very unlikely that the five that underwent IIF at T_h would lack any internal heterogeneous nucleators while the other 109 contained them. If one accepts that reasoning, one is lead to the conclusion that the heterogeneous nucleator for the other 109 is external ice that has penetrated into the egg interior as a consequence of the appearance of a defect in the plasma membrane during cooling.

Why would the membrane develop a defect during cooling that allows EI to penetrate? It seems unlikely that it is due to the attainment of a critically high m_s since the m_s at the mean flash temperature varies from 0.45 to 3.0 molal; i.e., 6-fold (Table 5). The flash

temperature, and hence m_s at the flash temperature, varies considerably more for individual oocytes in a given solution as depicted in Figs. 3 and 4. It seems unlikely that individual cells would inherently vary that much with respect to sensitivity to m_s.

Similarly, U at the mean flash temperature varies from 0.04 to 0.23 for a given solution, also a 6-fold ratio and L varies from 0.04 to 0.31, nearly 8-fold. The variation for individual oocytes in given solutions also varies considerably.

Differences between Xenopus and mouse oocytes

Examination of Table 6 and other comparisons we have made show that there are major differences in the IIF responses of *Xenopus* and mouse oocytes; namely:

(i) While both show a decrease in IIF temperature with increase in CPA concentration, the effect is much stronger in the mouse than in *Xenopus*. Also, *Xenopus* shows a peculiar difference between EG and glycerol with respect to the range of concentrations over which there is an effect (Fig. 5). Although the difference is statistically significant ($p < 0.01$), we have no explanation for it.
(ii) In mouse oocytes, the mean flash temperatures of oocytes in 1.0 and 1.5 M EG and glycerol approach or lie at T_h. In *Xenopus* oocytes, all the mean flash temperatures lie well above T_h, although as we have pointed out, five of the *Xenopus* oocytes flashed at T_h.
(iii) In mouse oocytes, flashing tended to occur within a narrow range of unfrozen fractions (U and L) [14]. That was not the case in *Xenopus*.

Comparison of IIF in Xenopus oocytes with that in other non-mammalian oocytes

Köseoglu et al. [8] reported for starfish oocytes and Hagedorn et al. [3] for zebrafish embryos that IIF as visualized by cryomicroscopy occurs at temperatures very close to that of EIF; i.e., they behave like *Xenopus* high-temperature flashers. On the other hand, embryos of two insect species, *Drosophila melanogaster* [16,13] and *Anopheles gambiae* [23] undergo IIF as measured by differential thermal analysis or DSC in a rather narrow range (−27 to −34 °C for *Drosophila*; −29 to −31 °C for *Anopheles*). The embryos of these two insect species differ in an important way from the starfish and zebrafish; namely, the surface of the two insect eggs are covered by water-impermeable barriers. This means that their underlying plasma membranes can not come in direct contact with external ice, if present. Indeed, their intracellular freezing temperatures are nearly the same whether their surfaces are briefly dried before cooling or whether external water (and ice) is present. However, the water-impermeable barrier around the *Drosophila* egg can be removed by appropriate treatment with alkanes [9,11]. When that is done, the mean intra-embryonic freezing occurs at a considerably higher temperature than in normal intact eggs [16]; i.e., −18 °C for permeabilized eggs in insect Ringers vs. −28 °C in intact eggs. When permeabilized eggs are frozen in 1 M EG at 16 °C/min, the IIF temperature again drops to −28 °C. The nucleation temperatures are somewhat lower than those reported here for the low-temperature *Xenopus* flashers (Tables 5 and 6).

Conclusions

We have indicated a number of factors that do not correlate with the IIF temperatures of Stage I and II *Xenopus* oocytes. What then is the determining factor(s)? There are a number of possibilities:

(1) The plasma membranes of individual oocytes could differ in their stability when faced with the several events occurring during cooling.
(2) Our assumption that none of the oocytes contain heterogeneous nucleators (an assumption based on the fact that 5 out of 114 do not) could be in error. Perhaps most oocytes do contain nucleators of varying effectiveness.
(3) If our conclusion that extracellular ice is the nucleator of intracellular ice correct, the ability of EI to induce defects in the plasma membrane and pass through it may depend on the intimacy of contact between the EI and the surface of a given oocyte. The local degree of intimacy may vary more than is reflected by the values of U and L, which are global quantities derived from the phase diagrams. It is important to note, that only a single defect of appropriate size would be required to provide a pathway for EI into the cell interior. In this regard, it is interesting that in a great majority of cases in *Xenopus*, flashing originated from a point source near the cell surface.

(4) Somewhat related to 3, above is that the intracellular ice nucleation temperature of a cell may be at least partly related to the size of the cell, perhaps because a larger cell distorts the extracellular ice lattice more than does a smaller cell. The only evidence we have that cell size may matter is (a) Kleinhans et al.'s [7] finding from DSC measurements that Stage V and VI oocytes undergo IIF at much higher temperatures than the much smaller Stage I and II oocytes, and (b) the fact that Stage I and II *Xenopus* oocytes undergo IIF at considerably higher temperatures than the still much smaller mouse oocyte. Of course with respect to (a), the development from Stage II to V involves more than just an increase in size of the egg. For example, yolk formation begins at Stage III and an increasing proportion of the cytoplasm is converted to yolk by Stages V and VI so that by these stages, the yolk occupies 80–90% of the cytoplasm (R.A. Wallace, personal communication; [25]).

References

[1] C.A. Angell, Supercooled water, in: F. Franks (Ed.), Water—A Comprehensive Treatise, vol. 7, 1982, pp. 8–11.

[2] R.M. Dean, R.L. Rivers, M.L. Zeidel, D.M. Roberts, Purification and functional reconstitution of soybean nodulin 26: an aquaporin with water and glycerol transport properties, Biochemistry 38 (1999) 347–353.

[3] M. Hagedorn, A. Peterson, P. Mazur, F.W. Kleinhans, High ice-nucleation temperature of zebrafish embryos: slow-freezing is not an option, Cryobiology 49 (2004) 181–189.

[4] P. Hausen, M. Riebesell, The Early Development of *Xenopus laevis*, Springer-Verlag, New York, 1991.

[5] M. Kasai, K. Ito, K. Edashige, Morphological appearance of the cryopreservaed mouse blastocyst as a tool to identify the type of cryoinjury, Human Reprod. 17 (2002) 1863–1874.

[6] F.W. Kleinhans, J.F. Guenther, S. Seki, K. Edashige, D.M. Roberts, P. Mazur, Water P_f of *Xenopus* (AQP +/−) Stage I and II oocytes, Cryobiology 51 (2005) 389.

[7] F.W. Kleinhans, J.F. Guenther, D.M. Roberts, P. Mazur, Analysis of intracellular ice nucleation in *Xenopus* oocytes by differential scanning calorimetry, Cryobiology 52 (2006) 128–138.

[8] M. Köseoglu, A. Eroglu, M. Toner, K.C. Sadler, Starfish oocytes form intracellular ice at unusually high temperatures, Cryobiology 43 (2001) 248–259.

[9] D.V. Lynch, T.-T. Lin, S.P. Myers, S.P. Leibo, R.J. MacIntyre, R.E. Pitt, P.L. Steponkus, A two-step method for permeabilization of *Drosophila* eggs, Cryobiology 26 (1989) 445–452.

[10] P. Mazur, Principles of cryobiology, in: B.J. Fuller, N. Lane, E.E. Benson (Eds.), Life in the Frozen state, CRC Press, Boca Raton, 2004, pp. 3–65.

[11] P. Mazur, K.W. Cole, A.P. Mahowald, Critical factors affecting the permeabilization of *Drosophila* embryos by alkanes, Cryobiology 29 (1992) 210–239.

[12] P. Mazur, I.L. Pinn, S. Seki, F.W. Kleinhans, K. Edashige, Effects of hold time after extracellular ice formation on intracellular freezing of mouse oocytes, Cryobiology 51 (2005) 235–259.

[13] P. Mazur, U. Schneider, A.P. Mahowald, Characteristics and kinetics of subzero chilling injury in *Drosophila* embryos, Cryobiology 29 (1992) 39–68.

[14] P. Mazur, S. Seki, I.L. Pinn, F.W. Kleinhans, K. Edashige, Extra- and intracellular ice formation in mouse oocytes, Cryobiology 51 (2005) 29–53.

[15] A. Melinder, Thermophysical properties of liquid secondary refrigerants, IIR, 1997.

[16] S.P. Myers, R.E. Pitt, D.V. Lynch, P.L. Steponkus, Characterization of intracellular ice formation in *Drosophila melanogaster* embryos, Cryobiology 26 (1989) 472–484.

[17] D.E. Pegg, Simple equations for obtaining melting points and eutectic temperatures for the ternary system glycerol/sodium chloride/water, Cryo-Letters 4 (1983) 268–269.

[18] R.I. Pozner, M.L. Shepard, F.H. Cocks, The equilibrium and non-equilibrium thermal behavior of aqueous ternary solutions based on complex physiological support media, containing NaCl, and dimethyl sulfoxide or glycerol, J. Mater. Sci. 12 (1977) 299–304.

[19] Quick, H.A. Lester, Methods for expression of excitability proteins in *Xenopus* oocytes, Methods Neurosci. 19 (1994) 261–279.

[20] W.F. Rall, P. Mazur, H. Souzu, Physical–chemical basis of the protection of slowly frozen human erythrocytes by glycerol, Biophys. J. 23 (1978) 101–120.

[21] W.F. Rall, P. Mazur, J.J. McGrath, Depression of the ice-nucleation temperature of rapidly cooled mouse embryos by glycerol and dimethyl sulfoxide, Biophys. J. 41 (1983) 1–12.

[22] D. Rasmussen, A.P. MacKenzie, Effects of solute on the ice-solution interfacial free energy; calulation from measured homogeneous nucleation temperatures, in: H.H.G. Jellinek (Ed.), Water Structure at the Water–Polymer Interface, Plenum, New York, 1972, pp. 126–145.

[23] P.D. Schreuders, E.D. Smith, K.W. Cole, M.-P. Valencia, A. Laughinghouse, P. Mazur, The characterization of intraembryonic freezing in *Anopheles gambiae* embryos, Cryobiology 33 (1996) 487–501.

[24] M.T. Valentine, Z.E. Perlman, T.J. Mitchs, D.A. Weitz, Biophys. J. 88 (2005) 680–689.

[25] R.A. Wallace, Studies on amphibian yolk III. A resolution of yolk platelet components, Biochim. Biophys. Acta 74 (1963) 495–504.

[26] E.J. Woods, M.A.J. Zieger, D.Y. Gao, J.K. Critser, Equations for obtaining melting points for the ternary system ethylene glycol/sodium chloride/water and their application to cryopreservation, Cryobiology 38 (1999) 403–407.

Available online at www.sciencedirect.com
ScienceDirect
CRYOBIOLOGY
Cryobiology 53 (2006) 160–168
www.elsevier.com/locate/ycryo

Expression of aquaporin-3 improves the permeability to water and cryoprotectants of immature oocytes in the medaka (*Oryzias latipes*) ☆

Delgado M. Valdez Jr., Takao Hara, Akira Miyamoto, Shinsuke Seki, Bo Jin, Magosaburo Kasai, Keisuke Edashige *

Laboratory of Animal Science, College of Agriculture, Kochi University, Nankoku, Kochi 783-8502, Japan

Received 20 December 2005; accepted 15 May 2006
Available online 22 June 2006

Abstract

The permeability of the plasma membrane plays a crucial role in the successful cryopreservation of oocytes and embryos. Several efforts have been made to facilitate the movement of water and cryoprotectants across the plasma membrane of fish oocytes/embryos because of their large size. Aquaporin-3 is a water/solute channel that can also transport various cryoprotectants. In this study, we tried to improve the permeability of immature medaka (*Oryzias latipes*) oocytes to water and cryoprotectants by artificially expressing aquaporin-3. The oocytes were injected with aquaporin-3 cRNA and cultured for 6–7 h. Then, hydraulic conductivity (L_P) and cryoprotectant permeability (P_S) were determined from volume changes in a hypertonic sucrose solution and various cryoprotectant solutions, respectively, at 25 °C. The L_P value of the cRNA-injected oocytes was 0.22 ± 0.04 μm/min/atm, nearly twice larger than that of intact or water-injected oocytes (0.14 ± 0.02 and 0.14 ± 0.03 μm/min/atm, respectively). P_S values of intact oocytes for ethylene glycol, propylene glycol, and DMSO were 1.36 ± 0.34, 1.97 ± 0.20, and 1.17 ± 0.52 × 10^{-3} cm/min, respectively. The permeability to glycerol could not be calculated because oocytes remained shrunken in the glycerol solution. On the other hand, cRNA-injected oocytes had significantly higher P_S values (glycerol, 2.20 ± 1.29; ethylene glycol, 2.98 ± 0.36; propylene glycol, 3.93 ± 1.70; DMSO, 3.11 ± 0.74 × 10^{-3} cm/min) than intact oocytes. When cRNA-injected oocytes were cultured for 12–14 h, 51% matured to the metaphase II stage, and 43% of the matured oocytes were fertilized and hatched following *in vitro* fertilization and 14 days of culture. Thus, the permeability of medaka oocytes to water and cryoprotectants was improved by the artificial expression of aquaporin-3, and the oocytes retained the ability to develop to term.

Keywords: Medaka; Aquaporin; Oocyte; Cryoprotectant; Water; Permeability

Long-term storage of embryos is useful for managing stocks of model organisms, and has been used for several mammalian species. However, the cryopreservation of freshwater fish embryos has not succeeded because several factors are suspected to

☆ This work was supported by Grants-in-Aid for scientific research from the Ministry of Education, Culture, Sports, Science, and Technology of Japan.
* Corresponding author. Fax: +81 88 864 5200.
E-mail address: keisuke@cc.kochi-u.ac.jp (K. Edashige).

0011-2240/$ - see front matter © 2006 Elsevier Inc. All rights reserved.
doi:10.1016/j.cryobiol.2006.05.003

complicate the process [19]. Fish embryos have a large volume, a large amount of egg-yolk, and a thick chorion, form a complex structure during development, and are susceptible to chilling. Among these factors, the size of the embryo may be the most serious obstacle to cryopreservation. Since large cells have a very low surface/volume ratio, the movement of water and cryoprotectants across the plasma membrane takes a long time. Consequently, the cells can be seriously damaged by the intracellular formation of ice, the toxicity of the cryoprotectant, and osmotic swelling during the process of cryopreservation and removal of cryoprotectants. Thus, the rapid movement of water and cryoprotectants through the membrane is essential for the cryopreservation of fish embryos.

In a previous study, we showed in the medaka, *Oryzias latipes*, that immature oocytes have several advantages for cryopreservation over mature oocytes and embryos [23]. Medaka oocytes acquire the ability to resist osmotic changes during the final stages of maturation and the volume changes of matured oocytes in hypertonic and hypotonic solutions are smaller than those of immature oocytes. On the other hand, immature oocytes respond to osmotic changes as expected and their plasma membrane and chorion are more permeable to water and cryoprotectants [23]. Moreover, it is known in zebrafish embryos that, soon after the 50–70% epiboly stage, the yolk is surrounded by the multinucleated yolk syncytial layer, which is a barrier to cryoprotectants [6]. However, fish oocytes are constituted from only a single compartment and do not have such barriers, although they too have features that complicate cryopreservation, i.e., a large size and the presence of a large amount of yolk. Since medaka sperm can be cryopreserved easily [1], long-term storage of this species could be realized if the cryopreservation of the oocyte became possible. However, in our previous study [23], we suggested that the permeability of immature oocytes is not sufficiently high for cryopreservation.

To overcome problems with the cryopreservation of fish oocytes and embryos, efforts have been made to introduce cryoprotectants into fish embryos under negative pressure [17], under hydrostatic pressure [20], by direct microinjection into the cytoplasm [13], and by dechorionation [5]. Another approach is to modify the permeability of the plasma membrane. In the 1990s, water channels, called aquaporins (AQPs), were discovered and characterized [14]. The channels occur in two groups: one is highly selective for water and the other transports not only water but also neutral solutes with a small molecular weight, such as cell-permeating cryoprotectants. In zebrafish embryos, AQP3, which acts as a water/cryoprotectant channel, can be artificially expressed and its expression improves the permeability to water and propylene glycol [7]. The artificial expression of AQP1, a channel selective for water, has also been shown to improve tolerance to freezing in yeast [21]. We have already demonstrated that the artificial expression of AQP3 in mouse oocytes achieved by the injection of its cRNA, increases their permeability to water and glycerol and that this improves the tolerance of the oocytes to cryopreservation [4]. Thus, the expression of such water channels in immature fish oocytes, which have greater permeability to water and cryoprotectants than matured oocytes and embryos, might further improve membrane-permeability.

In this study, we tried to artificially express AQP3, a water/cryoprotectant channel, in immature medaka oocytes in order to increase the permeability of the plasma membrane to water and cryoprotectants.

Materials and methods

Preparation of aquaporin-3 cRNA

AQP3 cRNA was synthesized as described elsewhere [4]. Briefly, AQP3 cDNA was cloned from rat kidney cDNA by polymerase chain reaction (PCR): the sense strand was 5′-CGGGATCCCAT GGGTCGACAGAAGGAGTT-3′, and the antisense strand was 5′-GCTCTAGAGGGTTTTA TGGGGTGTCC-3′ (underlined sequences indicate inserted *Bam*HI and *Xba*I sites, respectively). These primers were derived from the rat AQP3 sequence [2] (Genbank™ Accession No. L35108). The PCR cycle had the following profile: 94 °C for 1 min, 58 °C for 2.5 min, and 72 °C for 2.5 min for 30 cycles. The PCR product contained the open reading frame of AQP3. The *Bam*HI/*Xba*I fragment of the PCR product was subcloned into the *Bgl*II/*Xba*I site of pSP64T (a gift from Dr. Paul A. Krieg), a *Xenopus* expression plasmid. After digestion of the construct by *Eco*RI (Toyobo, Osaka, Japan), capped cRNA of AQP3 was synthesized using SP6 polymerase (Takara Shuzo, Otsu, Japan). *Bam*HI, *Xba*I and *Bgl*II were obtained from New England Biolabs (Beverly, MA, USA).

Immature oocytes with or without aquaporin-3 cRNA microinjection

About 20–100 matured orange-red type medaka, purchased from a local fish dealer, were maintained in 60-l aquaria under 14-h light and 10-h dark periods at 26 °C. Fully grown oocytes with 0.8–0.9 mm in diameter were obtained as immature oocytes from ovaries of actively spawning females humanely killed 1–3 h before the start of the dark period, and placed in 15 ml of 90% TCM 199 with Earle's salts (Cat. No. 31100-035, Gibco Invitrogen Corp., Carlsbad, CA, USA) (90% TCM-199) [11] in a Petri dish (90 × 10 mm) at 25 °C for 2–4 h prior to use. Then, an oocyte was held with a holding pipette connected to a micromanipulator on an inverted microscope and injected with about 60 nl of water (a control) or AQP3 cRNA solution (1 ng/nl) with an injection needle connected to another micromanipulator. As another control, non-injected intact oocytes were used. Both injected and non-injected oocytes were cultured in an incubator at 25 °C for 6–7 h (until the germinal vesicle break down stage) in 90% TCM-199. Only a limited number of oocytes were used in each experiment because the period of culture for expression of AQP3 was limited to 6–7 h.

Permeability of oocytes to water and cryoprotectants

Oocytes cultured in 90% TCM-199 for 6–7 h were introduced into 90% TCM-199 containing 0.89 M sucrose or 90% TCM-199 containing a cryoprotectant (200 μl) covered with paraffin oil in a Petri dish (35 × 10 mm) for 1 h at 25 ± 1 °C, with a minimal amount of 90% TCM-199 using a pipette. The microscopic images of the oocytes were recorded using a time lapse video recorder (ETV-820, Sony, Tokyo, Japan) for 1 h. The cross sectional area of the oocyte was measured using an image analyzer (VM-50, Olympus, Tokyo, Japan). Relative cross sectional area, S, is expressed by dividing it by the initial area of the same oocyte. The relative volume was obtained from $V = S^{3/2}$. Hydraulic conductivity (L_P) and cryoprotectant permeability (P_S) were determined by fitting water and solute movements using the two-parameter formalism [16] as described elsewhere [4,23]. In one experiment, the volume changes of oocytes in 90% TCM-199 containing 0.89 M sucrose were measured at 15 °C and the L_P was determined. We calculated the Arrhenius activation energy for the permeability to water of oocytes from Arrhenius plots by use of the L_P values at two points (15 and 25 °C). The L_P and P_S values for each cryoprotectant were calculated from volumetric changes in 90% TCM-199 containing 0.89 M sucrose and that containing 10% (v/v) glycerol, 8% (v/v) ethylene glycol, 10% (v/v) propylene glycol, or 9.5% (v/v) DMSO. The osmolalities contributed by sucrose, glycerol, ethylene glycol, propylene glycol, and DMSO were 1.23, 1.59, 1.61, 1.56, and 1.55 Osm/kg, respectively, excluding the osmolality contributed by 90% TCM-199 (0.27 Osm/kg). The osmolalities of sucrose, glycerol, ethylene glycol, and propylene glycol were calculated from published data on the colligative properties of each cryoprotectant in aqueous solutions [27]. The osmolality of 9.5% DMSO in an aqueous solution was measured with a vapor pressure osmometer (Vapro 5520; Wescor Inc., Logan, UT, USA) and that of 90% TCM-199 was measured with a freezing point depression osmometer (OM801; Vogel, Giessen, Germany). The total osmolality of each solution used is shown in Table 1. Various other constants and parameters are listed in Table 2.

Table 1
The osmolality of solutions used

Diluent		Solute (Osm/kg)		Total osmolality (Osm/kg)
Basic medium	Osmolality[a] (Osm/kg)	Name	Osmolality	
90% TCM-199	0.27	—	—	0.27
	0.27	0.89 M sucrose	1.23[b]	1.50
	0.27	10% glycerol	1.59[b]	1.86
	0.27	8% ethylene glycol	1.61[b]	1.88
	0.27	10% propylene glycol	1.56[b]	1.83
	0.27	9.5% DMSO	1.55[c]	1.82

[a] Osmolality measured with a freezing point depression osmometer.
[b] Osmolality calculated from published data on the colligative properties of the solutes in aqueous solutions [27].
[c] Osmolality measured with a vapor pressure osmometer.

Table 2
Constants and parameters used for fitting permeability parameters

Symbol	Meaning	Values
R	Gas constant (liter atm K^{-1} mol^{-1})	8.206×10^{-2}
T	Absolute temperature	298 K
$\bar{V}_W$	Partial molar volume of water	0.018 l/mol
$\bar{V}_{GLY}$	Partial molar volume of glycerol[a]	0.071 l/mol
$\bar{V}_{EG}$	Partial molar volume of ethylene glycol [a]	0.054 l/mol
$\bar{V}_{PG}$	Partial molar volume of propylene glycol[a]	0.070 l/mol
$\bar{V}_{DMSO}$	Partial molar volume of DMSO[b]	0.069 l/mol
$\bar{V}_b$	Osmotically inactive volume[c]	0.41

[a] From Wolf et al. [27].
[b] From Kiyohara et al. [15].
[c] From Valdez et al. [23].

The volume percentage was varied to prepare cryoprotectant solutions with similar osmolality.

We assumed that the osmolality of the oocyte cytoplasm was equilibrated with that of 90% TCM-199 (0.27 Osm/kg) because, until used for experiments, oocytes were cultured in 90% TCM-199 for 6–7 h, a period sufficient for the oocytes to be equilibrated with the medium.

Developmental ability of aquaporin-3 cRNA-injected oocytes

We regarded oocytes as 'matured' and 'fertilized' from their appearance [10]. Intact and AQP3 cRNA-injected oocytes were matured by being cultured in 90% TCM-199 at 26 °C for 14 h [11]. Oocytes matured to the metaphase II stage were inseminated using a modified version of Yamamoto's method [12,28], and fertilized oocytes were developed in Hanks solution [26]. Briefly, testes obtained from two mature males were transferred into 1 ml of saline formulated for medaka oocytes (SMO medium) (0.24 Osm/kg) at room temperature. The composition of the solution was as follows; NaCl, 6.50 g; KCl, 0.40 g; $CaCl_2 2H_2O$, 0.15 g; $MgSO_4 7H_2O$, 0.15 g; $NaHCO_3$, 1.00 g; Phenol Red, 0.015 g; in 1 l of aqueous solution with 5 mM Hepes–HCl, pH 7.0 [9]. Sperm were released from the testis by tearing it with forceps and the solution was used as the sperm suspension. Five to twenty matured oocytes were transferred into a dish (35 × 10 mm) with a minimal amount of 90% TCM-199 using a pipette, and were inseminated by adding 200 μl of the sperm suspension. After 5 min, 4 ml of Hanks' balanced solution was added to the dish. Then, we incubated the oocytes at 26 °C for 1 h and observed them under a stereomicroscope to distinguish fertilized from unfertilized oocytes. Fertilized eggs were transferred to Hanks' balanced solution containing 3 μg/l of methylene blue, and then incubated at 26 °C for 14 days. Hatching was regarded as a criterion for full development.

Statistics

The L_P and P_S of intact oocytes, water-injected oocytes, and AQP3 cRNA-injected oocytes were compared with the Student's t-test, and the developmental ability of intact oocytes and AQP3 cRNA-injected oocytes was compared with a χ^2 test ($P < 0.05$ was considered significant).

Results

Permeability to water of aquaporin-3 cRNA-injected oocytes

Fig. 1 shows changes in the volume of oocytes in 90% TCM-199 containing 0.89 M sucrose at 25 °C. Intact and water-injected oocytes shrunk slowly and did not differ in volume change, suggesting that water-injected oocytes have the same low-permeability as intact oocytes. On the other hand, AQP3 cRNA-injected oocytes shrunk more rapidly, sug-

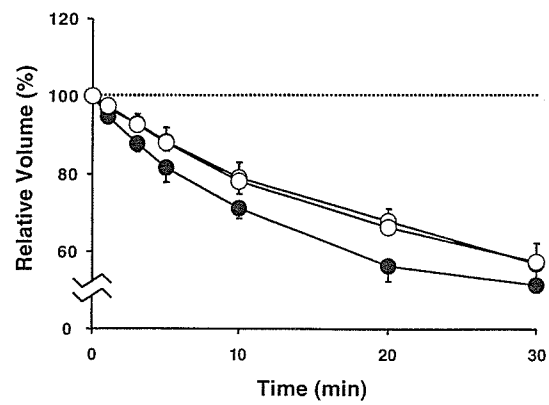

Fig. 1. Change in cell volume of intact immature oocytes (open circles) and water (shaded circles) or aquaporin-3 cRNA-injected (closed circles) immature oocytes in a hypertonic sucrose solution. Intact oocytes and water- or AQP3 cRNA-injected oocytes were cultured in 90% TCM-199 medium (0.27 Osm/kg) at 27 °C for 6–7 h. Then, they were exposed to 90% TCM-199 containing sucrose (1.50 Osm/kg) at 25 °C for 1 h. Data are indicated as means of relative volumes ± SD. Data on intact, water-injected and AQP3 cRNA-injected oocytes were from 12, 11, and 9 oocytes, respectively.

gesting that the permeability to water had increased. The mean for the L_P of cRNA-injected oocytes was 0.22 ± 0.04 μm/min/atm, nearly twice larger than that for intact or water-injected oocytes (0.14 ± 0.02 or 0.14 ± 0.03 μm/min/atm, respectively) (Table 3). The Arrhenius activation energy of intact oocytes was high (11.0 kcal/mol) but that of cRNA-injected oocytes was low (5.5 kcal/mol) (Table 3). These results indicate that AQP3 cRNA-injected oocytes expressed AQP3 and that artificial expression of AQP3 enhanced the permeability to water of medaka immature medaka oocytes.

Table 3
Permeability of immature medaka oocytes to water

Oocyte	L_P (μm/min/atm)[a]		E_a[b] (kcal/mol)
	15 °C	25 °C	
Intact	0.07 ± 0.02	0.14 ± 0.02	11.0
Water-injected	n.d.[c]	0.14 ± 0.03	n.d.[c]
AQP3 cRNA-injected	0.16 ± 0.03	0.22 ± 0.04**	5.5

[a] Hydraulic conductivity.
[b] Arrhenius activation energy of water-permeability.
[c] Not determined.
** Significantly different from intact oocytes at 25 °C (Student's t-test, $P < 0.01$).

Since the permeability of water-injected oocytes did not differ from that of intact oocytes, we used only intact oocytes as controls in the experiments that followed.

Permeability to cryoprotectants of aquaporin-3 cRNA-injected oocytes

Fig. 2 shows volume changes of intact and AQP3 cRNA-injected oocytes in 90% TCM-199 containing 10% glycerol, 8% ethylene glycol, 10% propylene glycol, or 9.5% DMSO at 25 °C for 1 h. In the glycerol solution, intact oocytes shrunk slowly and did not regain their volume during the 1-h exposure period, suggesting that glycerol permeates intact oocytes quite slowly (Fig. 2A). Since we did not observe a re-swelling phase during the period of exposure, we could not calculate the permeability to glycerol of intact oocytes. In the ethylene glycol, propylene glycol and DMSO solutions, intact oocytes shrunk but regained their volume thereafter (Figs. 2B–D), suggesting that these cryoprotectants permeated the intact oocytes. P_{EG}, P_{PG}, and P_{DMSO} values were 1.36 ± 0.34, 1.97 ± 0.20, and $1.17 \pm 0.52 \times 10^{-3}$ cm/min, respectively (Table 4). On the other hand, AQP3 cRNA-injected oocytes

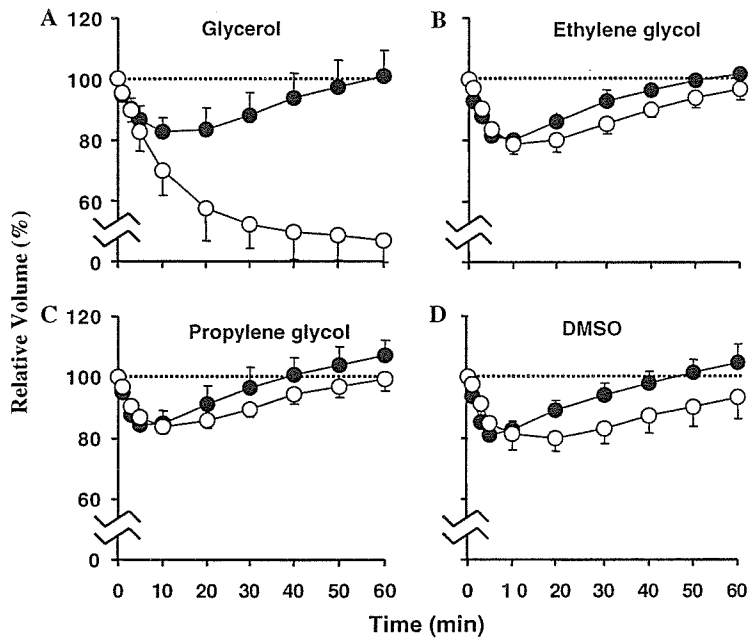

Fig. 2. Change in cell volume of intact (open circles) and aquaporin-3 cRNA-injected (closed circles) immature oocytes in 10% glycerol (A), 8% ethylene glycol (B), 10% propylene glycol (C), and 9.5% DMSO (D) solutions. Oocytes were exposed to 90% TCM-199 medium containing a cryoprotectant at 25 °C for 1 h. Data are indicated as means of relative volumes ± SD. Each curve in (A–D) was based on 9–10 oocytes.